Article

Persistent vegetation greening trends across China's wetlands

Check for updates

Yongxing Ren[1], Dehua Mao[1] ✉, Tao Wang [2], Mohamed Abdalla[3], Pete Smith [3], Xiangming Xiao [4], Zicheng Yu[1], Xiuxue Chen[5], Yanbiao Xi[1], Ling Luo[1], Xiaoyan Li[6] & Zongming Wang[1]

Vegetation is the basic component of wetland ecosystems. Monitoring changes in aboveground biomass (AGB) of wetland vegetation is crucial for understanding the response of wetland ecosystems to global climate change. China has vast wetlands experiencing diverse climate change impacts. However, how the AGB of wetland vegetation responds to climate change and human impacts remains unclear. This lack of understanding stems from insufficient in-situ observations, complex interactions between wetland vegetation growth and local hydrology, and challenges in estimating AGB using remote sensing data alone. Here, we compiled a wetland AGB dataset with 1087 sites covering all wetland regions in China (639 sample points from field sampling and 448 sample points from literature). Based on this dataset, we mapped the spatial distribution of wetland AGB in China using machine learning algorithms to understand its historical and future changes. The wetland AGB density of China in 2020 was 352.23 ± 32.67 g C m^{-2} on average and the total wetland AGB stock was 57.51 ± 6.36 Tg C. During the past two decades (2000–2023), wetland AGB has gradually increased, indicating a notable greening trend in China's wetlands. Our results project that China's wetlands could continue to green-up rapidly and sustainably under various future climate change scenarios, but with varying degrees of greening. This highlights the difference in wetland ecosystem response to various climate conditions.

Wetland has the highest carbon sequestration capacity per unit area of all ecosystems, which is crucial to mitigating global warming[1–3]. The aboveground biomass (AGB) of wetland vegetation is a pivotal indicator of ecosystem response to climate change. Accurately assessing AGB is the fundamental basis for estimating the carbon sequestration potential of wetland ecosystems[4,5]. However, monitoring the spatial-temporal changes in wetland vegetation AGB remains a major challenge in the carbon cycle research[6,7]. Given the critical importance of wetland changes in coping with climate change and the poor characterization of wetland AGB changes, it is imperative to rigorously monitor the dynamic changes of wetland AGB with precision and accuracy.

China is renowned for its vast expanse of natural and diverse wetland types. Assessing wetland AGB has drawn particular attention in recent decades[8,9]. Although many studies have evaluated wetland AGB at local to regional scales, few studies have examined the current pattern of historical change and projected future trends of wetland AGB at a national scale under

climate change[10]. The study of large-scale wetland AGB is often constrained by factors such as the sparsity of in situ AGB observations, the availability of wetland types and area data, and the accuracy of predictive models. National inventory surveys of wetland AGB require great input from human power and other resources. Although inventory monitoring of AGB can be compensated for by remote sensing techniques and local surveys[11,12], the lack of consistent large-scale wetland distribution data also limited the accuracy of wetland AGB estimation. Considerable efforts have been devoted to estimating large-scale wetland AGB using a robust spatiotemporal projection model[13,14]. Spatial interpolation methods, such as kriging and inverse distance weighting (IDW), have provided rapid mapping techniques for wetland AGB based on field sampling[15]. However, these approaches are limited in capturing temporal variations in wetland AGB. To address this, vegetation indices derived from surface reflectance data have emerged as essential covariates for wetland AGB estimation[16]. The normalized difference vegetation index (NDVI) and enhanced vegetation index (EVI) positively

[1]State Key Laboratory of Black Soils Conservation and Utilization, Northeast Institute of Geography and Agroecology, Chinese Academy of Sciences, Changchun, China. [2]State Key Laboratory of Tibetan Plateau Earth System, Resources and Environment (TPESRE), Institute of Tibetan Plateau Research, Chinese Academy of Sciences, Beijing, China. [3]Institute of Biological and Environmental Sciences, University of Aberdeen, Aberdeen, UK. [4]School of Biological Sciences, Center for Earth Observation and Modeling, University of Oklahoma, Norman, OK, USA. [5]School of Geographical Sciences, Changchun Normal University, Changchun, China. [6]College of Earth Science, Jilin University, Changchun, China. ✉e-mail: maodehua@iga.ac.cn

correlate with AGB, making them widely used and effective for AGB estimation[17]. Due to the widespread distribution and diverse vegetation types in wetlands, spectral variations exist among different vegetation types. In addition, the presence of water could profoundly impact the spectrum signal. Consequently, studies relying exclusively on a single vegetation index for AGB estimation in large-scale or highly diverse regions often produce unsatisfactory results[18]. Machine learning algorithms have been proven suitable for predicting wetland AGB, particularly for large-scale or diverse sample datasets[19,20]. Machine learning algorithms can effectively integrate remote sensing observations and other geographic data. These algorithms are also valuable tools for establishing spatial projection models of wetland AGB and for accurately evaluating the spatial-temporal changes of wetland AGB.

Understanding the dynamics of wetland AGB is important for assessing ecosystem responses to climate change. Climate change and anthropogenic disturbances have been identified as the primary drivers for inter-annual variations in wetland AGB[21]. Previous studies have well documented that higher temperatures stimulate vegetation photosynthesis, leading to an increase in wetland AGB[22,23]. Conversely, reduced precipitation constrains vegetation growth, resulting in a decline in AGB[24,25]. Previous studies have extensively explored the spatial distribution in wetland AGB under various climatic conditions[15]. These analyses about the influencing factors of vegetation AGB within a timeframe may result in overlooking the response of AGB to long-term climate change. Moreover, variations in AGB are also influenced by shifts in vegetation types, which can be attributed to natural ecosystem evolution and human activities[4,26]. Long-term dynamics and future trends in wetland AGB, under the combined influence of those factors, remain unclear.

This study aimed to assess the spatial pattern of wetland AGB and its historical and future changes on a national scale in China. In this study, we compiled a wetland AGB database integrating AGB observations from field surveys and data collected from the literature. Different machine learning algorithms were applied to develop an effective wetland AGB model. The optimal model was then used to understand the spatial distribution of wetland AGB in China and to evaluate and project the effects of historical and future climate change on wetland AGB.

Results
Model development and evaluation for wetland AGB
Our results of different statistical models showed that the random forest model, incorporating vegetation indices, environmental variables, and wetland types, demonstrated the best AGB predictive performance, with an R^2 value of 0.82 and relative error (RE) of 14.65% (Fig. 1). Machine learning models that utilize multiple covariates outperformed autoregressive and single-factor models in terms of accuracy. Linear and power function models based on individual vegetation indices exhibited lower accuracy, with R^2 values below 0.3. Among the autoregressive models, the ordinary kriging (OK) model achieved an R^2 value of 0.39, higher than IDW and nearest-neighbor interpolation (NeI). The machine learning models showed varying accuracies depending on the employed covariates. Model accuracy was improved by including environmental and vegetation-type covariates. When considering machine learning models with the same set of covariates, the random forest model outperformed multivariate linear regression, extreme gradient boosting (XGBoost), support vector machine (SVM) models, and convolutional neural network models in accuracy. Hence, a random

Fig. 1 | Regressive results for estimating wetland AGB. Vegetation indicators include NDVI, EVI, MSAVI, RVI, and WDVI. Environmental covariates included elevation, slope, temperature, and precipitation. Weighted difference vegetation index (WDVI), ratio vegetation index (RVI), modified soil adjusted vegetation index (MSAVI), inverse distance weighting (IDW), nearest-neighbor interpolation (NeI), extreme gradient boosting (XGBoost), support vector machine (SVM), and ordinary kriging (OK), and relative error (RE).
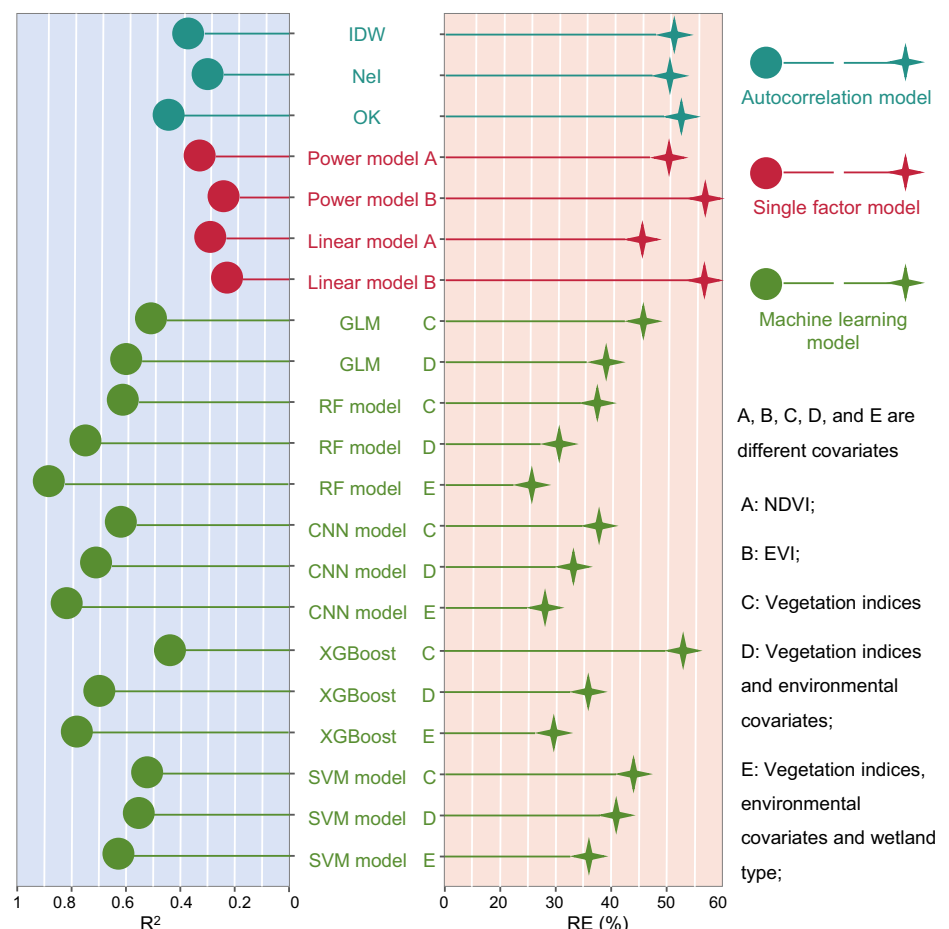
Fig. 2 | Spatial pattern of wetland AGB in China. **a** Spatial distribution of wetland AGB. The lower left histogram insets show the area proportions of different AGB levels. **b** Wetland AGB and area at different latitudes.
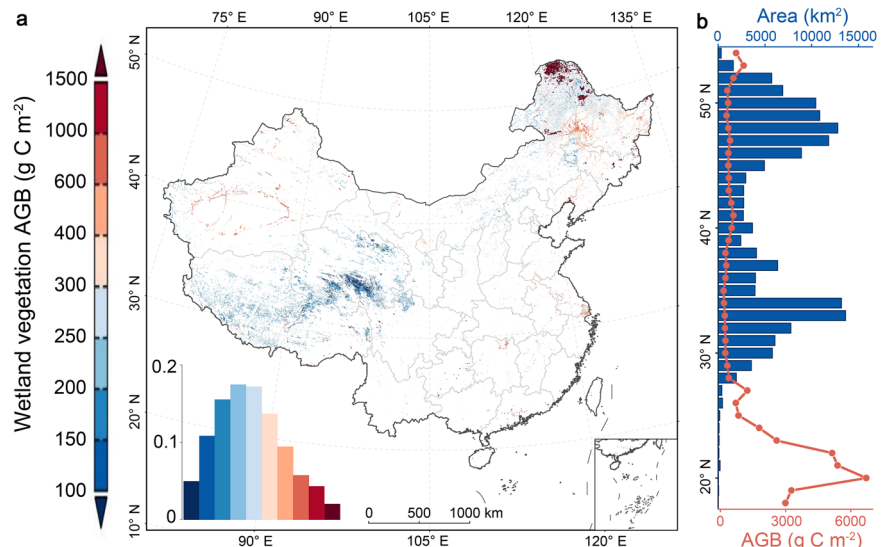
forest model incorporating vegetation indices, environmental variables, and vegetation types was selected for this study to estimate wetland AGB in China.

Spatiotemporal changes of wetland AGB in China

The spatial pattern of the wetland AGB generated using a random forest model showed that the average wetland AGB in China was 352.23 ± 32.67 g C m^{-2}, with over 70% of the regions having AGB values below 400 g C m^{-2} (Fig. 2). We observed that the wetland AGB decreased with increasing latitude and elevation (Fig. 3). The AGB increased with annual precipitation. The large spatial gradient in temperature and precipitation across wetlands in China led to interregional differences in wetland AGB, with the highest value (3442.75 ± 451.29 g C m^{-2}) in the Southeast and South China region and the lowest one (244.76 ± 18.52 g C m^{-2}) on the Tibetan Plateau.

Our results indicated that the wetland AGB stock in China was 57.51 ± 6.36 Tg C. We also observed considerable variations in AGB in terms of wetland type (Fig. 4). Quantitative analysis of the area and AGB of different wetland types in China revealed certain discrepancies between the proportions of area and AGB. The highest AGB density was found in coastal swamps (5978.98 ± 615.14 g C m^{-2}). However, as coastal swamps accounted for only 0.2% of the total wetland area, they contributed 3.6% (2.04 Tg C) of AGB to the total China's wetlands. Inland swamps accounted for only 5.1% of the total wetland area, but they contributed over 20% (57.51 ± 6.36 Tg C) of the wetland AGB stock in China (Fig. 4). The lowest AGB density was found in the inland marsh (274.18 ± 26.86 g C m^{-2}). Inland marsh area was the dominant wetland type in China, occupying 93% of the wetland area, whilst it contributed to 72.3% (41.56 Tg C) of the wetland AGB stock.

History changes of wetland vegetation AGB

The average wetland AGB from 2000 to 2023 was estimated to be approximately 345.52 ± 26.87 g C m^{-2} (Fig. 5a). In terms of temporal changes in the AGB of wetlands across China, there was an overall increasing trend of 1.29 ± 0.14 g C m^{-2} yr^{-1} in the past two decades. The increase was more pronounced in the northern part of the northeastern region and the southeastern coastal area. In terms of latitude, both high latitudes (greater than 50 degrees) and low latitudes (lower than 20 degrees) exhibited a higher growth rate compared to the other regions (Fig. 6). Among the different regions, the Southeast and South China region exhibited a pronounced increase in wetland AGB change rate. In contrast, the Inner Mongolia–Xinjiang Plateau and Lower and middle reaches of Yellow River regions showed a decreasing trend. Other regions showed a slight increase (Supplementary Fig. 1a). The change rate of

wetland AGB gradually decreased with increasing elevation, with a change rate of 4.52 g C m^{-2} yr^{-1} in areas below 200 meters and a decrease to -1.54 g C m^{-2} yr^{-1} in areas above 3000 m (Supplementary Fig. 1b). The change rate of wetland AGB demonstrated a positive correlation with temperature and precipitation, suggesting that a higher temperature and more precipitation resulted in a greater positive change rate of wetland AGB (Supplementary Figs. 1c, d).

Projected future changes in wetland AGB across China

Different future climate scenarios led to distinct changes in the wetland AGB (Fig. 5b). In the Shared Socioeconomic Pathway 126 (SSP126) scenario, the wetland AGB in China will be relatively stable, with an average value of 356.52 ± 26.38 g C m^{-2} for the 2024–2100 period. The wetland AGB exhibited a slight increasing trend under the Shared Socioeconomic Pathway 245 (SSP245) scenario, with a growth rate of 0.21 ± 0.02 g C m^{-2} yr^{-1} and an average value of 365.65 ± 34.75 g C m^{-2} for the 2024–2100 period. In contrast, the Shared Socioeconomic Pathway 585 (SSP585) scenario projected a notable increase in wetland AGB compared to the current levels, with an even more pronounced increase after 2060, projected to exceed 400 g C m^{-2} by 2100. Spatial variations in wetland AGB were observed under different climate change scenarios (Fig. 7). In the SSP126 scenario, the AGB change rate in wetland vegetation was relatively small. The SSP245 scenario exhibited a increase in the AGB change rate compared to the SSP126 scenario, especially in the northern part of the Northeast China. In contrast, the SSP585 scenario demonstrated a considerably higher and more prominent AGB change rate. Regions with a positive AGB change rate accounted for 80%, with over 40% of the areas exceeding 1 g C m^{-2} per year. Across different latitudes, the wetland AGB stock change rate was higher in the SSP585 scenario than in the SSP126 and SSP245 scenarios. A higher AGB stock change rate was observed around 30 degrees and 50 degrees.

Discussion

We compiled a AGB dataset for China's wetlands comprising 1087 samples (Supplementary Data 1), covering various wetland ecosystems nationwide. Multi-year field sampling efforts were conducted between 2009 and 2021 to collect the data. Additionally, literature data was employed, incorporating data from various sources published between January 2000 and May 2023. This comprehensive dataset helped overcome the limitations of data availability in previous studies[27]. We selected a wetland extent dataset known for its good data consistency and high classification accuracy (China_wetlands) to estimate wetland AGB and its variations[8]. Furthermore, we performed comprehensive evaluations of the widely used models for estimating wetland AGB, from which we selected the model with the
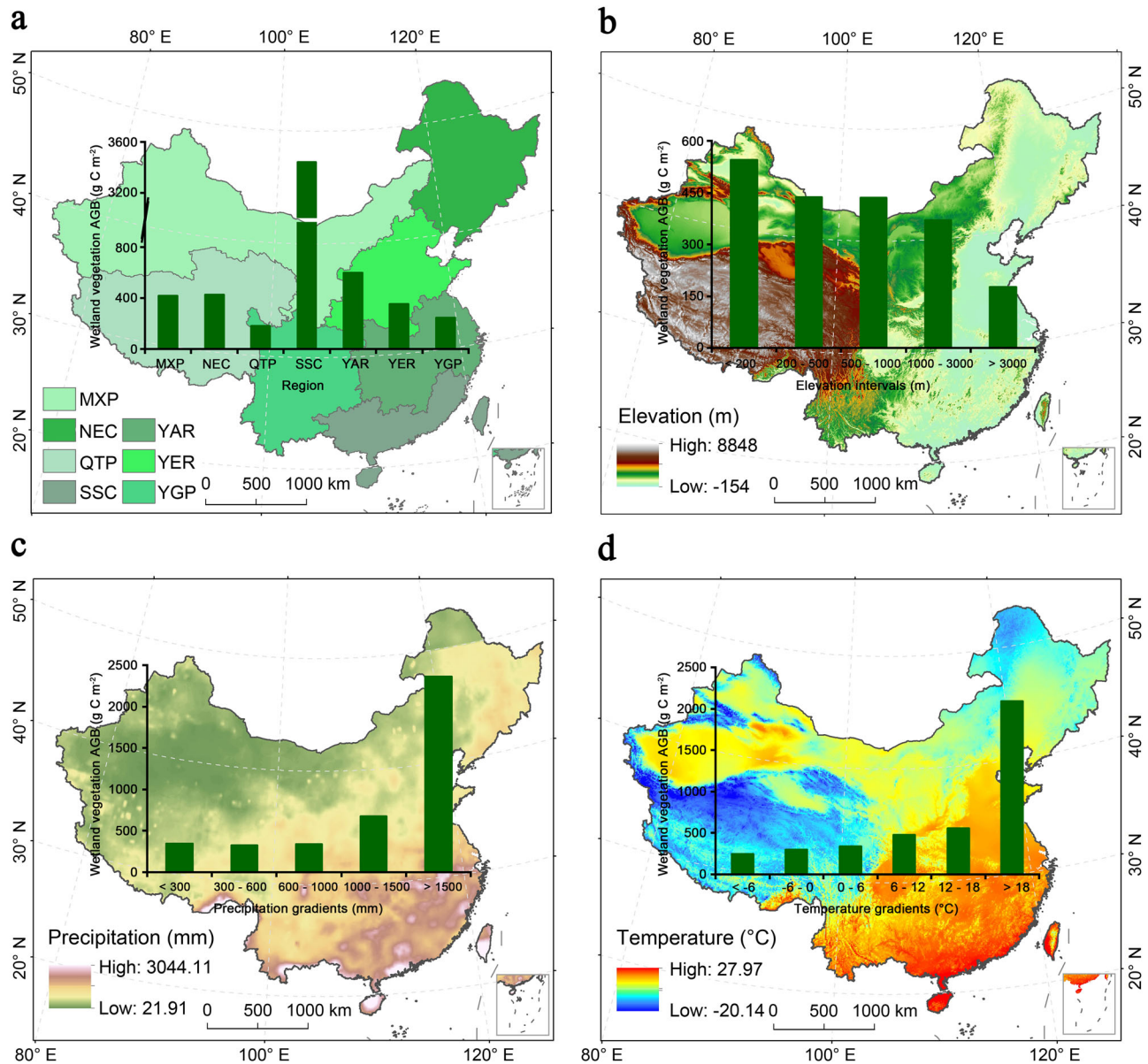
Fig. 3 | The variation in averaged wetland AGB in different geographic regions. a Average wetland AGB in different regions. **b** Average wetland AGB at different elevation intervals. **c** Average wetland AGB in different precipitation gradients. **d** Average wetland AGB in different temperature gradients.

best performance to enhance our estimation accuracy. Traditional autocorrelation-based spatial interpolation models showed relatively poor performance, given the weak spatial correlation between samples and the nonzonal distribution pattern of wetlands[28]. Remote sensing vegetation indices could not accurately reflect the reflectance information of wetland vegetation due to the influence of wetland hydrology. Therefore, the accuracy of the simple linear regression model was extremely limited[18]. Careful consideration of multiple environmental factors is critical in wetland AGB modeling to improve model accuracy. The random forest model can adequately capture the complex relationship between wetland AGB and various spectral indices and environmental factors. This result demonstrates its ability to accommodate non-linear relationships between wetland AGB and multiple covariates while minimizing model errors. This study ensured precise projections by meticulously considering the data and methodology.

Due to the limited availability of extensive wetland survey data, research on the spatial distribution and dynamic change of wetland AGB in China has been lacking[11]. We presented an unprecedented analysis of China's wetland AGB at a national scale using a machine learning approach, employing a constructed national dataset of wetland AGB alongside wetland

distribution data. This study generated a spatial distribution map of wetland AGB in China. Its interannual variations were evaluated, providing a supplement to existing wetland AGB maps or sample measurements. We also forecast the future change and analyzed the historical change and current pattern of wetland AGB. This study conducted a quantitative analysis to assess the impacts of various carbon emission scenarios on wetland AGB, and thus enhanced our understanding of temporal changes in wetland AGB and greening. Expanding this knowledge is crucial for understanding the response of wetland ecosystems to global change.

Our study findings revealed an estimated wetland AGB of $352.23 \pm 32.67\,\mathrm{g\,C\,m^{-2}}$, with inland marshes exhibiting slightly lower measurements at $274.18 \pm 26.86\,\mathrm{g\,C\,m^{-2}}$. These results were slightly higher than the AGB estimation of marshes provided by Shen et al. $(227.5\,\mathrm{g\,C\,m^{-2}})$[15]. This discrepancy can likely be attributed to variations in the timing of the estimates and differences in the methods used. On the one hand, Shen et al.'s dataset was a field survey sample from 2013 to 2017, while the data sample in this study spanned over 20 years. On the other hand, the machine learning method was adopted in this study to draw the spatial and temporal distribution of AGB more accurately in

China's wetlands, rather than the kriging interpolation method used by Shen et al.[15]. Differences in the use of wetland data may also be one of the reasons for the variance in the estimation of wetland AGB. Various
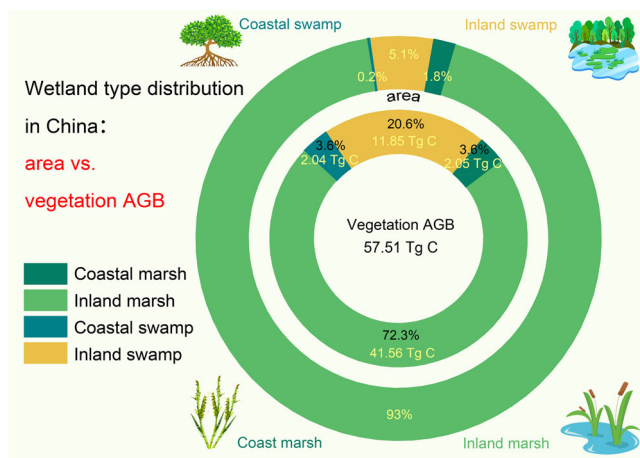

Fig. 4 | Area proportion and vegetation AGB proportion in different wetland types. Outer ring for AGB density and inner ring for AGB stock. Coastal marsh: natural wetland with dominant herbaceous vegetation in coastal areas. Coastal swamp: natural wetland with dominant woody vegetation in coastal areas including forested wetland and shrub wetland. Inland marsh: natural wetland with dominant herbaceous vegetation in inland areas. Inland swamp: natural wetland with dominant woody vegetation in inland areas including forested wetland and shrub wetland.

topographic and climatic conditions have strongly influenced the spatial distribution of wetland AGB in China. In areas such as the Qinghai–Tibet Plateau, characterized by high elevation and low temperatures, the wetland AGB was considerably lower compared to other geographic regions in China. Conversely, the humid climate of the southeast coastal area contributed to a higher wetland AGB compared to different geographic regions. Variations in wetland vegetation types also played a role in AGB differences, with swamps exhibiting notably greater AGB than marshes. The northern part of Northeast China was particularly interesting, where wetland AGB was surprisingly high despite the high elevation and low temperature. This result can be attributed primarily to the extensive distribution of inland swamps in this area. These findings are consistent with previous small-scale studies, which support the idea that vegetation AGB tends to be higher in the southeast coastal area and lower in the Qinghai–Tibet Plateau region[10,29,30].

Previous studies demonstrated that the global vegetation had an evident greening in recent years, and pronounced greening was observed both in China and India due to afforestation and agricultural intensification, respectively[31,32]. Our study confirmed that Chinese wetlands also exhibited a greening trend. While the greening of cultivated and woody lands was primarily driven by human impacts, the causes of wetland greening and AGB increases in China were likely subject to the combined influences of climate change and human activities. The feature importance results from the random forest model indicated that wetland type and climate had a strong influence on wetland AGB density (Supplementary Fig. 2). Therefore, the greening of wetland vegetation was sensitive to changes in temperature and precipitation. Over the past two decades, both temperature and precipitation within Chinese wetland areas exhibited a general increasing trend. Warming and wetting climates, in combination with enriched

Fig. 5 | Temporal variation of wetland AGB.
a Historical changes in AGB from 2000 to 2023. **b** Future trends of AGB from 2024 to 2100 under different climate scenarios. Shaded areas represent the 95% confidence intervals.
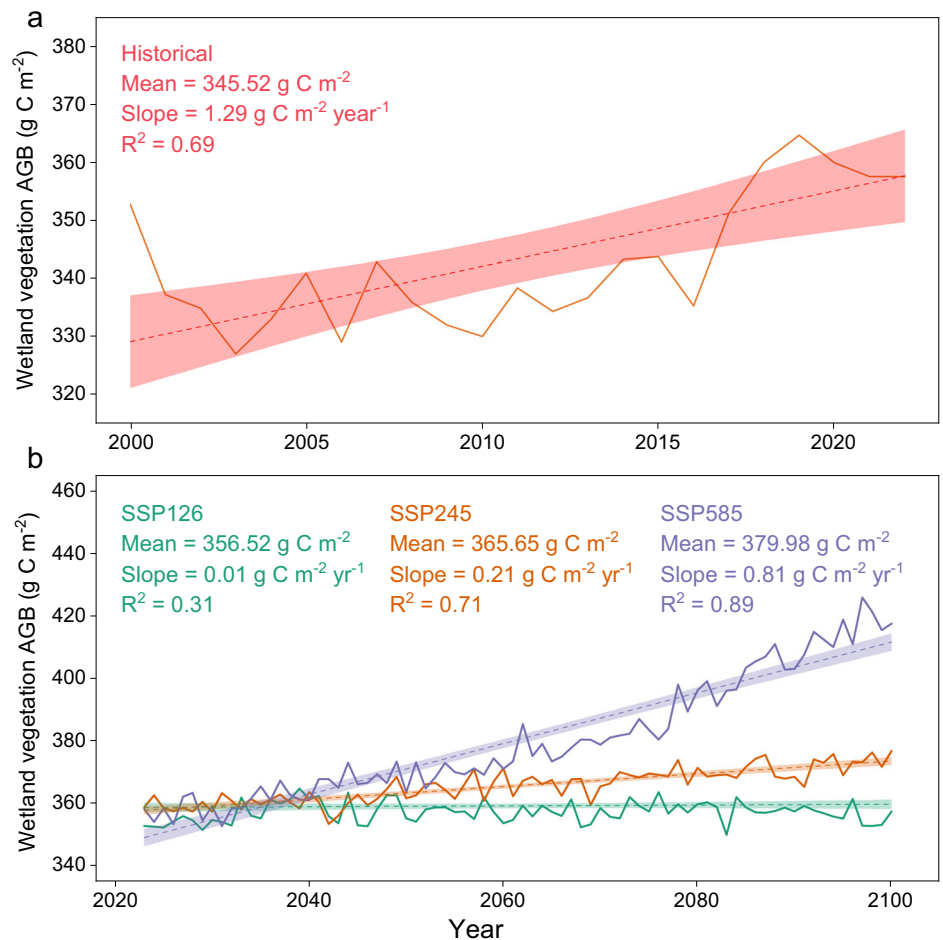
Fig. 6 | Spatial patterns of temporal changes in wetland AGB across China from 2000 to 2023. a Spatial distribution of wetland AGB change. The lower left histogram insets show the area proportions of different AGB change levels. **b** Wetland AGB changes and area at different latitudes.
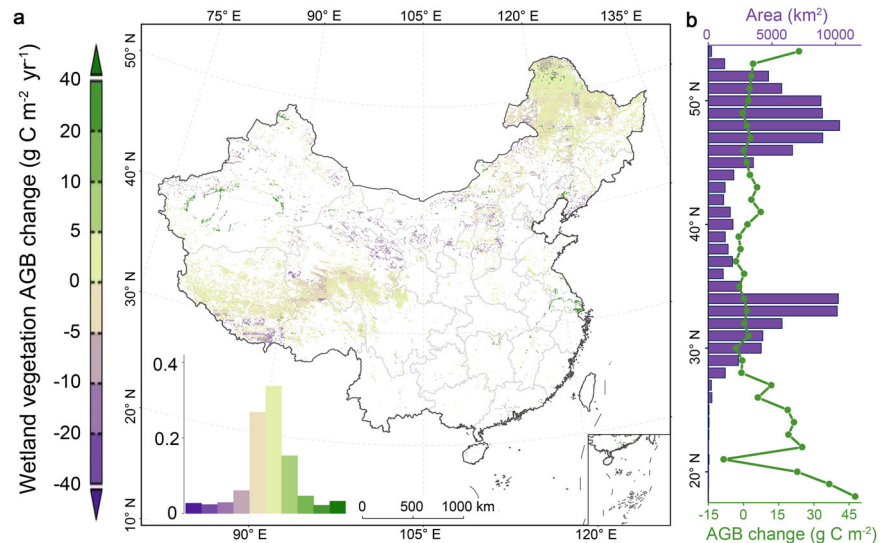
atmospheric CO_2, have obvious positive effects on the growth of vegetation and promote the greening of wetlands[31,33]. Similarly, the greening of wetland may be affected by atmospheric nitrogen deposition. The recent increase in atmospheric nitrogen deposition has enhanced plant photosynthetic capacity and stimulated plant growth, potentially resulting in increased wetland AGB[34,35]. Similar wetland greening trends were also observed worldwide under global warming[22,36,37]. On the mid-Atlantic coast, increasing temperature and precipitation in recent years promoted the wetland greening[22]. Warming has also stimulated vegetation growth in northern peatlands, thus promoting wetland greening[37].

The greening of wetland vegetation in China was not only influenced by climate change, but may also have been positively affected by human activities. AGB density showed marked differences among different wetland vegetation types, and wetland type was the most important driving factor in the random forest model. Therefore, changes in wetland types driven by human activities had a substantial impact on the greening trend of vegetation. On one hand, the increasing emphasis on wetland protection and progressively improved conservation systems resulted in reduced negative disturbances from human activities such as grazing and drainage[8]. China's recent shift from wetland exploitation to restoration and protection may have contributed substantially to wetland greening[38]. On the other hand, vegetation community changes within wetlands also positively contributed to this greening process. The Chinese government has extensively planted mangroves and other coastal swamps in the Southeast and South China region, with a higher AGB than coastal marshes[39]. The area of mangroves has rapidly expanded in recent years, and as mangroves grow, the AGB of the vegetation increases accordingly[40]. In addition to the plantation of mangroves in the Southeast and South China region, the invasion of alien species, such as the *Spartina alterniflora* in the Lower and middle reaches of Yellow River region, also has a substantially impact[41]. Changes in wetland communities, such as the expansion of high-biomass community types like *Spartina alterniflora*, led to increases in wetland AGB.

The historical changes observed in wetland AGB suggest that climate change will likely drive alterations in wetland AGB. The effect of future climate change on wetland AGB was substantial in this study (Figs. 5 and 7). This study quantitatively analyzed the impact of different SSP scenarios on wetland AGB. The changes in wetland AGB remained relatively stable over time under the SSP126 scenario. The SSP245 scenario, characterized by increased carbon emissions, showed a slight upward trend in vegetation AGB. In contrast, the SSP585 scenario exhibited a substantial increase in vegetation AGB, with a more pronounced trend after 2060 and a projected 10% increase by 2100. This result indicated that, under the SSP245 and SSP585 scenarios, China's wetlands are continuously and rapidly greening.

Different trends in temperature and precipitation in the future are expected to result in diverse trends in wetland AGB variation. Wetland plants can absorb and sequester a substantial amount of carbon dioxide, trapping it within the vegetation and soil. This process aids in mitigating CO_2 released into the atmosphere, contributing to climate mitigation efforts[42,43]. The increase in wetland AGB under the SSP585 scenario may enhance the carbon sequestration capacity of the wetland ecosystems. However, it is noteworthy that this context may also result in the loss of stored organic carbon in wetland soils, impacting ecosystem stability[11]. A deeper understanding of wetland AGB and greening changes can enhance our comprehension of ecosystem responses to climate change. In the face of climate change, we advocate for strengthened wetland management, with close attention to the variations in wetland AGB and greening, to better address future climate change challenges.

The results of this study showed that AGB density increased by 3.88% from 2000 to 2020 in the unchanged wetland. However, based on the mean value of wetland AGB density in these two years and considering wetland area changes between 2000 and 2020, the total wetland AGB stock decreased by 8.57% from 2000 to 2020. To enhance wetland protection, the Chinese government implemented a series of wetland conservation and restoration measures in recent years[39]. As a result, the decrease in wetland areas in China has slowed notably, and wetland areas in many areas are rebounding[8]. The expectation is that wetland area and wetland AGB stock in China will increase further.

While visual assessments and statistical testing of the models indicated that the estimates were reasonable, the inherent uncertainties and limitations of this study must be acknowledged. Firstly, we acknowledge several limitations in our current analysis regarding the impact of wetland area changes on AGB dynamics. Our assessment of historical AGB changes was exclusively based on unchanged wetlands from 2000 to 2020, thereby excluding the effects of wetland reclamation and restoration activities. Secondly, our projections of future AGB changes were based on the 2020 wetlands spatial distribution. Although China's wetland areas have remained relatively stable in recent years, the potential influence of future wetland area changes on AGB dynamics introduces additional uncertainty to our predictions. Furthermore, our environmental data framework, apart from climatic data, is anchored to 2020 baseline. This includes various vegetation indices that may undergo alterations in response to climate change. Finally, comprehensive quantitative assessment of human impacts was lacking. Future studies should prioritize establishing reliable datasets for these analyses and exploring anthropogenic influences on wetland AGB dynamics across broader geographical scales, extending to the global level.
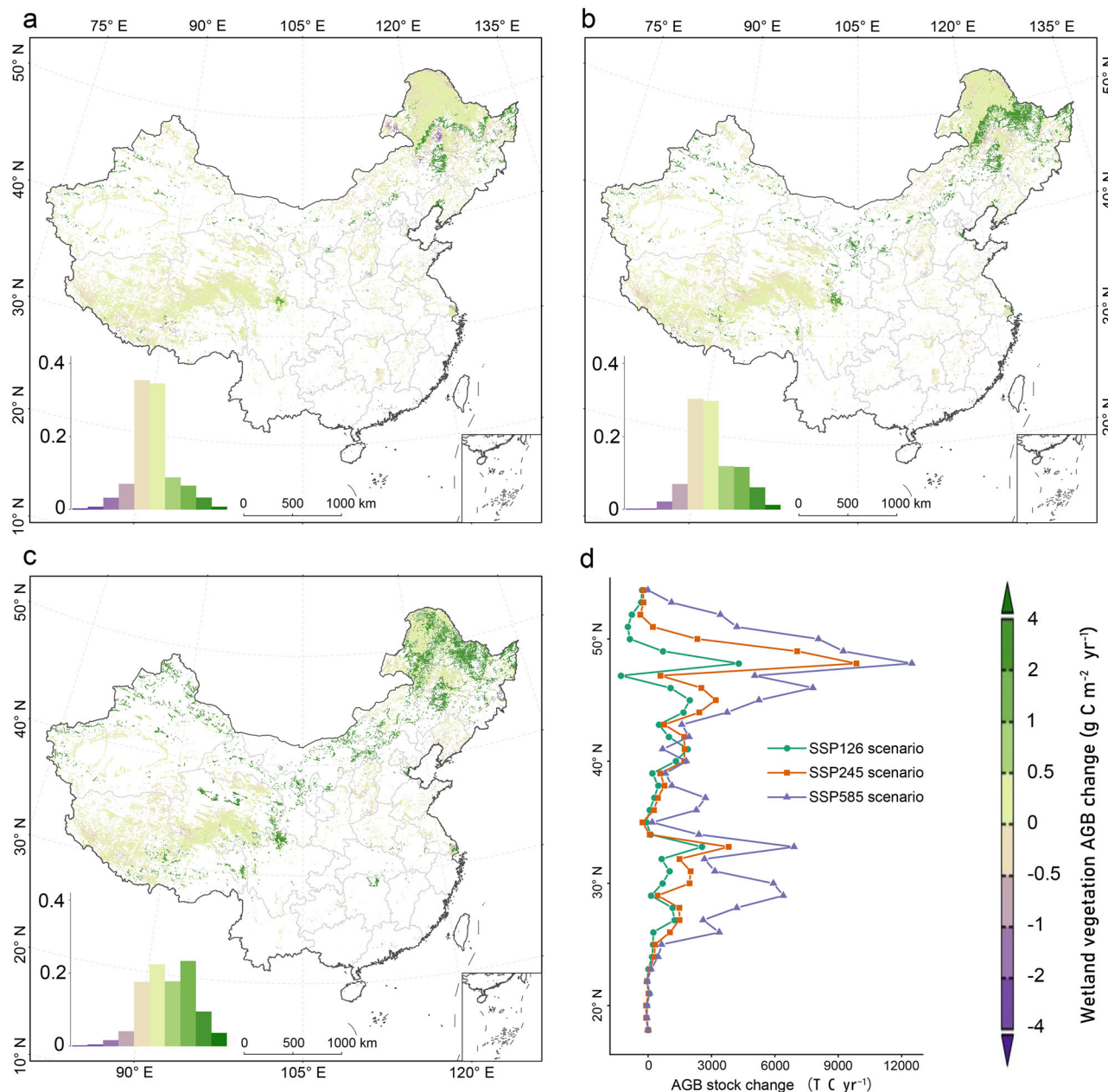
Fig. 7 | Spatial patterns of wetland AGB change in China from 2024 to 2100 under different future scenarios. a Spatial distribution of wetland AGB change under the SSP126 scenario. **b** Spatial distribution of wetland AGB change under the SSP245 scenario. **c** Spatial distribution of wetland AGB change under the SSP585 scenario. The lower left histogram insets in (**a–c**) show the area proportions of different AGB change levels. **d** Wetland AGB stock changes at different latitudes under different scenarios. Shared Socioeconomic Pathway 126 (SSP126), Shared Socioeconomic Pathway 245 (SSP245), and Shared Socioeconomic Pathway 585 (SSP585).

Date and methods

Wetland extent distribution

This study focused on vegetated natural wetlands, encompassing both inland and coastal types. To map wetland extent, we utilized the China_-Wetlands dataset[8]. This dataset offers robust wetland classification (overall accuracy: 95.1%), making it a valuable resource for such investigations. In 2020, the total wetland area across China was $162.8 \times 10^3 \, km^2$. Most of the wetlands are distributed in Northeast China and Qinghai–Tibet Plateau (Supplementary Fig. 3a). About 20% ($33.79 \times 10^3 \, km^2$) of wetlands in China experienced changes in terms of gains or losses during the past two decades, from 2000 to 2020. We investigated wetland AGB changes for seven geographic regions in China, specifically in this study[8], including Northeast China, Qinghai–Tibet Plateau, Yunnan–Guizhou Plateau, Inner

Mongolia–Xinjiang Plateau, Lower and middle reaches of Yellow River, Lower and middle reaches of Yangtze River, and Southeast and South China (Supplementary Fig. 3a).

Wetland AGB dataset

The AGB of different wetland types in this study refers to the total AGB of wetland vegetation per unit area. The term "marsh" refers to herbaceous wetlands dominated by grasses and reeds, while "swamp" denotes woody wetlands characterized by trees and shrubs. Their respective AGB represents the total vegetation biomass within these ecosystems' aboveground components, excluding belowground structures. We compiled AGB observations from two sources to generate the AGB dataset for China's wetlands, including in-situ observations from field surveys and data from the

literature. The in-situ observations include 639 sites collected from seven field surveys conducted from 2009 to 2021. These field surveys were conducted during August, with consistent and well-designed field sampling protocols that balance site uniformity, site accessibility, and costs. All the sample plots were surveyed with three replicates (0.5 m × 0.5 m) to obtain the mean value (1 m × 1 m) of the biomass[18]. The in-situ AGB samples were taken into the laboratory, oven-dried at 65 °C and then weighed with a precision of 0.01 g. Consistent with previous studies, a factor of 0.45 was adopted to convert vegetation biomass to carbon density in this study[44,45]. We also compiled wetland AGB records from peer-reviewed publications concerning wetlands in China. Publications between January 2000 and May 2023 were searched through the Web of Science, Google Scholar, and the China National Knowledge Infrastructure for Studies. The keywords used to search the studies included vegetation AGB, marsh, swamp, wetland, and China. If available, the main texts and supplementary files of these manuscripts were checked to identify the dataset with vegetation AGB measurements. Primary data were sourced either directly from published tables or, where tabular data were unavailable, derived by digitizing figures. This digitization utilized GetData Graph Digitizer (version 2021b; OriginLab Corporation) and (version 2.24; http://www.getdata-graph-digitizer.com/). These tools have demonstrated high digitization accuracy (>99%) and are widely used[46–48]. The literature dataset comprised 77 studies published from 2000 to 2023, with 448 sample points (Supplementary Fig. 3b). The final dataset obtained by the two methods included 1087 samples across China[49], covered all wetland types in China.

Covariate variables

Wetland AGB is influenced by climate, terrain, hydrology, and vegetation type[50]. Certain vegetation indices can effectively characterize vegetation wetland AGB[13,51]. Therefore, this research incorporates various geographic spatial data as covariates in the model for wetland AGB (Supplementary Table 1).

This study used MODIS surface reflectance products (MOD09A1, MOD11A2, and MOD113A1) from June 1st, 2000, to October 1st, 2023, archived in the Google Earth Engine cloud platform. The annual NDVI, EVI, weighted difference vegetation index (WDVI), ratio vegetation index (RVI), and modified soil adjusted vegetation index (MSAVI) were calculated from 2000 to 2023[52,53].

Elevation data at a spatial resolution of 250 meters were acquired from the Global Digital Elevation Model (US Geological Survey, http://glovis.usgs.gov/). Climatic data (temperature and precipitation) were sourced from the National Meteorological Information Center of China (NMICC, http://data.cma.cn/). To ensure spatial consistency with the other environmental variables, the original 1000 m resolution climate data were resampled to 250 m using the NEI method. Subsequently, the environmental attribute values (elevation, temperature, precipitation and vegetation index, etc.) corresponding to each raster cell were extracted to all sampling point locations. These spatially aligned values then served as inputs for the subsequent spatial analysis algorithms.

Future climate data were used to predict changes in wetland AGB. The future climate scenarios used in this study were obtained from the near-surface atmospheric drive datasets (https://cstr.cn/18406.11.Meteoro.tpdc.270998). The dataset includes projections from three different models, EC-Earth3, GFDL-ESM4, and MRI-esm2-0, covering the period from 2024 to 2100 under three different scenarios: SSP126 (low-carbon emissions), SSP245 (medium-carbon emissions), and SSP585 (high-carbon emissions)[54]. The average precipitation and temperature of the three models were computed using Matlab software (Matlab R2019a), and future climate data were resampled using the NeI method, with a spatial resolution of 250 m.

Data analysis process

Four main steps were performed to estimate wetland AGB in China. First, the in-situ wetland AGB dataset was established by combining field sampling and literature data. Second, multiple covariates, such as vegetation indices, climate variables, and topography, were preprocessed and integrated with the in-situ wetland AGB dataset. Third, different wetland AGB models were established, and the optimal model was selected to estimate wetland AGB based on the accuracy of the evaluations. Fourth, the current pattern, historical change, and projected future trends of wetland AGB were conducted based on historical environmental covariates and future climate data. Geospatial data downloading and processing were accomplished on the Google Earth Engine cloud platform, and models were established in R (version 4.0.2; https://www.r-project.org/). The flowchart of general data processing and analysis is shown in Supplementary Fig. 4.

Spatial extrapolation of wetland AGB

We compared the performance of the three types of models in estimating wetland AGB and selected an optimal model based on their accuracy in this study. The three types of models were (1) autocorrelation models. These models use the geographic locations of sample sites as explaining variables and extrapolate the in-situ AGB observations according to the distance of a target pixel to the data samples. IDW, NeI, and OK model were used in this study. (2) Regression models based on single vegetation indices and linear and power models. (3) Machine learning models. These models consider multiple covariates. We compared generalized linear, random forest, XGBoost, SVM models, and deep learning models. A total of 1087 samples were collected. Among these, 70% (761 samples) were randomly selected for model construction, while the remaining 30% (326 samples) were used for accuracy validation. The following metrics were employed to assess the accuracy of the projection models: R^2 and RE. Finally, the current pattern of wetland AGB in 2020 was reconstructed based on the selected optimal model.

Projections of historical change and future trends in wetland AGB

In our analysis of historical wetland AGB changes, we focused exclusively on wetland areas that remained unchanged from 2000 to 2020. Therefore, this study excluded AGB changes induced by wetland area changes. The wetland AGB in different years was reconstructed using the optimal model based on topographic data, vegetation type and historical covariate data (vegetation index and climate data from 2000 to 2023). In the future trends of wetland AGB, we only consider the impacts of climate changes on wetland AGB, with the wetland area fixed in 2020. Future climate data under different carbon emission scenarios were also used to predict future wetland AGB based on an optimal model. The annual mean value and change rate of wetland AGB were determined by analyzing the annual projection results. Similar to vegetation primary productivity and vegetation indices such as NDVI and EVI, we defined changes in AGB density as wetland greening dynamics.

Data availability

References

1. Batjes, N. H. Total carbon and nitrogen in the soils of the world. *Eur. J. Soil Sci.* **65**, 10–21 (2014).
2. Dargie, G. C. et al. Age, extent and carbon storage of the central Congo Basin peatland complex. *Nature* **542**, 86–90 (2017).

3. Song, S. et al. Mangrove reforestation provides greater blue carbon benefit than afforestation for mitigating global climate change. *Nat. Commun.* **14**, 756 (2023).

4. Temmink, R. et al. Recovering wetland biogeomorphic feedbacks to restore the world's biotic carbon hotspots. *Science*. **376** (2022).

5. Chopping, M. et al. Remote sensing of woody shrub cover in desert grasslands using MISR with a geometric-optical canopy reflectance model. *Remote Sens. Environ.* **112**, 19–34 (2008).

6. Serrano, O. et al. Australian vegetated coastal ecosystems as global hotspots for climate change mitigation. *Nat. Commun.* **10**, 4313 (2019).

7. Crooks, S. et al. Coastal wetland management as a contribution to the US National Greenhouse Gas Inventory. *Nat. Clim. Change* **8**, 1109–1112 (2018).

8. Mao, D. et al. The trajectory of wetland change in China between 1980 and 2020: hidden losses and restoration effects. *Sci. Bull.* **70**, 587–596 (2024).

9. Kirwan, M. L., Megonigal, J. P., Noyce, G. L. & Smith, A. J. Geomorphic and ecological constraints on the coastal carbon sink. *Nat. Rev. Earth Environ.* **4**, 393–406 (2023).

10. Wang, Y., Shen, X., Jiang, M., Tong, S. & Lu, X. Spatiotemporal change of aboveground biomass and its response to climate change in marshes of the Tibetan Plateau. *Int. J. Appl. Earth Observ. Geoinf.* **102**, 102385 (2021).

11. Zheng, Y., Niu, Z., Gong, P., Dai, Y. & Shangguan, W. Preliminary estimation of the organic carbon pool in China's wetlands. *Chin. Sci. Bull.* **58**, 662–670 (2013).

12. Ma, K. et al. Refining soil organic carbon stock estimates for China's palustrine wetlands. *Environ. Res. Lett.* **10**, 124016 (2015).

13. Byrd, K. B. et al. A remote sensing-based model of tidal marsh aboveground carbon stocks for the conterminous United States. *ISPRS J. Photogramm. Remote Sens.* **139**, 255–271 (2018).

14. Campbell, A. D., Fatoyinbo, L., Goldberg, L. & Lagomasino, D. Global hotspots of salt marsh change and carbon emissions. *Nature* **612**, 701–706 (2022).

15. Shen, X. J. et al. Aboveground biomass and its spatial distribution pattern of herbaceous marsh vegetation in China. *Sci. China* **64**, 1115–1125 (2021).

16. Santi, E. et al. The potential of multifrequency SAR images for estimating forest biomass in Mediterranean areas. *Remote Sens. Environ.* **200**, 63–73 (2017).

17. Kilpeläinen, A. et al. Net climate impacts of forest biomass production and utilization in managed boreal forests. *GCB Bioenergy.* **8**, 307–316 (2016).

18. Ren, Y. et al. Aboveground biomass of marshes in Northeast China: spatial pattern and annual changes responding to climate change. *Front. Ecol. Evolut.* **10**, 1–12 (2022).

19. O'Shea, R. E. et al. Advancing cyanobacteria biomass estimation from hyperspectral observations: Demonstrations with HICO and PRISMA imagery. *Remote Sens. Environ.* **266**, 112693 (2021).

20. Grimm, R., Behrens, T., Märker, M. & Elsenbeer, H. Soil organic carbon concentrations and stocks on Barro Bolorado Island—digital soil mapping using random forests analysis. *Geoderma* **146**, 102–113 (2008).

21. Gabler, C. A. et al. Macroclimatic change expected to transform coastal wetland ecosystems this century. *Nat. Clim. Change* **7**, 142–147 (2017).

22. Chen, Y. & Kirwan, M. L. Climate-driven decoupling of wetland and upland biomass trends on the mid-Atlantic coast. *Nat. Geosci.* **15**, 913–918 (2022).

23. Keenan, T. F. & Riley, W. J. Greening of the land surface in the world's cold regions consistent with recent warming. *Nat. Clim. Change* **8**, 825–828 (2018).

24. Wang, Y. et al. Aboveground biomass of wetland vegetation under climate change in the Western Songnen Plain. *Front. Plant Sci.* **13**, 941689 (2022).

25. Bardou, R. et al. Projected changes in mangrove distribution and vegetation structure under climate change in the southeastern United States. *J. Biogeogr.* **51**, 2285–2297 (2024).

26. Rocha, A. V. & Goulden, M. L. Why is marsh productivity so high? New insights from eddy covariance and biomass measurements in a Typha marsh. *Agric. For. Meteorol.* **149**, 159–168 (2009).

27. Wang, M. et al. Global soil profiles indicate depth-dependent soil carbon losses under a warmer climate. *Nat. Commun.* **13**, 5514 (2022).

28. Ren, Y. et al. Investigating spatial and vertical patterns of wetland soil organic carbon concentrations in China's Western Songnen plain by comparing different algorithms. *Sustainability* **12**, 932 (2020).

29. Zhao, Y. et al. Mapping phragmites australis aboveground biomass in the Momoge wetland Ramsar site based on Sentinel-1/2 Images. *Remote Sens.* **14**, 694 (2022).

30. Chen, J. M. Carbon neutrality: Toward a sustainable future. *Innovation* **2**, 100127 (2021).

31. Piao, S. et al. Characteristics, drivers and feedbacks of global greening. *Nat. Rev. Earth Environ.* **1**, 14–27 (2020).

32. Gui, Y. et al. Vegetation greenness in 2024. *Nat. Rev. Earth Environ.* **6**, 255–257 (2025).

33. Richardson, C. M. et al. The impacts of climate change on coastal groundwater. *Nat. Rev. Earth Environ.* **5**, 100–119 (2024).

34. Wang, D. et al. Effects of nutrient addition on degraded alpine grasslands of the Qinghai-Tibetan Plateau: a meta-analysis. *Agric. Ecosyst. Environ.* **301**, 106970 (2020).

35. Capek, P. T. et al. A plant-microbe interaction framework explaining nutrient effects on primary production. *Nat. Ecol. Evolut.* **2**, 1588–1596 (2018).

36. Song, Y., Jiao, W., Wang, J. & Wang, L. Increased global vegetation productivity despite rising atmospheric dryness over the last two decades. *Earth's. Future* **10**, e2021EF002634 (2022).

37. Chen, N. et al. Warming-induced vapor pressure deficit suppression of vegetation growth diminished in northern peatlands. *Nat. Commun.* **14**, 7885 (2023).

38. Li, H. et al. Invasion of Spartina alterniflora in the coastal zone of mainland China: control achievements from 2015 to 2020 towards the Sustainable Development Goals. *J. Environ. Manag.* **323**, 116242 (2022).

39. Mao, D. et al. Conversions between natural wetlands and farmland in China: a multiscale geospatial analysis. *Sci. Total Environ.* **634**, 550–560 (2018).

40. Jia, M. et al. Mapping global distribution of mangrove forests at 10-m resolution. *Sci. Bull.* **68**, 1306–1316 (2023).

41. Zhang, J. et al. Spartina alterniflora invasion benefits blue carbon sequestration in China. *Sci. Bull.* **69**, 1991–2000 (2024).

42. Nguyen, V. L., Palmer, L. & Stangoulis, J. Higher photochemical quenching and better maintenance of carbon dioxide fixation are key traits for phosphorus use efficiency in the wheat breeding line, RAC875. *Front. Plant Sci.* **12**, 816211 (2021).

43. McFarlane, C. R. et al. Structural basis of light-induced redox regulation in the Calvin-Benson cycle in cyanobacteria. *Proc. Natl. Acad. Sci. USA.* **116**, 20984–20990 (2019).

44. Lamlom, S. H. & Savidge, R. A. A reassessment of carbon content in wood: variation within and between 41 North American species. *Biomass Bioenergy* **25**, 381–388 (2003).

45. Fang, J., Guo, Z., Piao, S. & Chen, A. Terrestrial vegetation carbon sinks in China, 1981–2000. *Sci. China Ser. D Earth Sci.* **50**, 1341–1350 (2007).

46. He, X. et al. Global patterns and drivers of soil total phosphorus concentration. *Earth Syst. Sci. Data.* **13**, 5831–5846 (2021).

47. Tan, L. et al. Land use and land cover changes in coastal and inland wetlands cause soil carbon and nitrogen loss. *Global Ecol. Biogeograp.* 1-23 (2022).

48. Ren, Y. et al. China's wetland soil organic carbon pool: New estimation on pool size, change, and trajectory. *Glob. Change Biol.* **29**, 6139–6156 (2023).

49. Ren Y. Persistent vegetation greening trends across China's wetlands. figshare. Dataset. https://doi.org/10.6084/m9.figshare.29352908.

50. Xu, C. et al. Remote Sensing-based Spatiotemporal Distribution of Grassland Aboveground Biomass and Its Response to Climate Change in the Hindu Kush Himalayan Region. *Chin. Geograph. Sci.* **32**, 759–775 (2022).

51. Gideon Neba, S., Kanninen, M., Eba'a Atyi, R. & Sonwa, D. J. Assessment and prediction of above-ground biomass in selectively logged forest concessions using field measurements and remote sensing data: case study in South East Cameroon. *For. Ecol. Manag.* **329**, 177–185 (2014).

52. Phillips, R. L. & Beeri, O. Scaling-up knowledge of growing-season net ecosystem exchange for long-term assessment of North Dakota grasslands under the Conservation Reserve Program. *Glob. Change Biol.* **14**, 1008–1017 (2008).

53. Clevers, J. G. P. W. Application of a weighted infrared-red vegetation index for estimating leaf Area Index by Correcting for Soil Moisture. *Remote Sens. Environ.* **29**, 25–37 (1989).

54. Zhang Lei PANX. Future climate projection of China based on regcm4.6 (2007-2099). (ed *National Tibetan Plateau Data C*). (National Tibetan Plateau Data Center, 2020).

Acknowledgements

Author contributions

Y.R., D.M. and Z.W. conceptualized the project, acquired funding and conducted investigations, and collated published wetland AGB data. Y.R. developed and conducted the model simulations and analysis with support from D. M., Z.W., X.C., Y. X., L.L. and X.L., and drafted the manuscript with contributions from all co-authors. D.M., T.W., M.A., P.S., Z.Y., X.X. and Z.W. participated in the discussion and analysis of the results and edited the manuscript. All authors reviewed the results, revised, and approved the manuscript.

Competing interests

The authors declare no competing interests.

Additional information